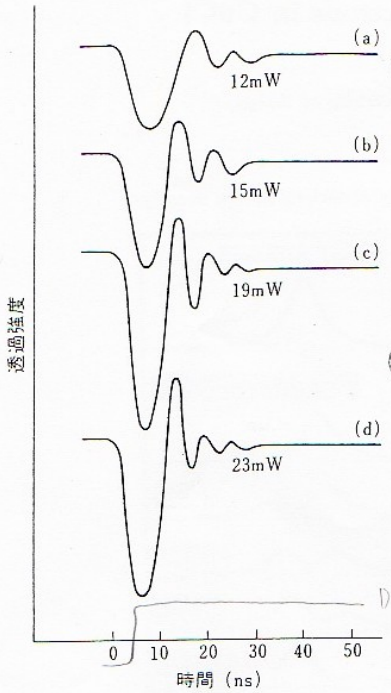

図2·8　ナトリウム蒸気を透過した光の強度をレーザー出力の関数として示す．(W. R. MacGillivray ら，文献 8 による．)

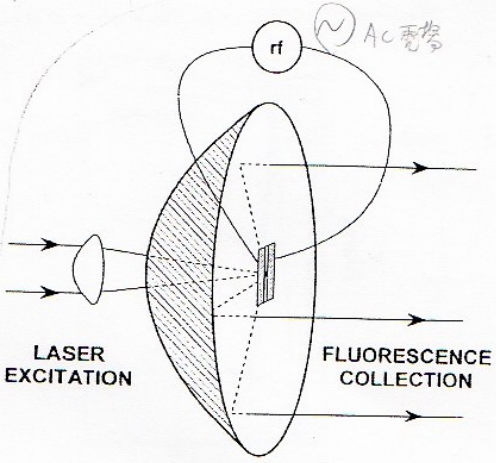

FIG. 1. Schematic diagram of the optical setup used to excite single molecules and to collect their fluorescence. The exciting laser is focused by a lens through a hole in a parabolic collecting mirror onto the sample placed on the front face of the mirror. The Stark shifting rf field is applied via two aluminum electrodes 18 μm apart.

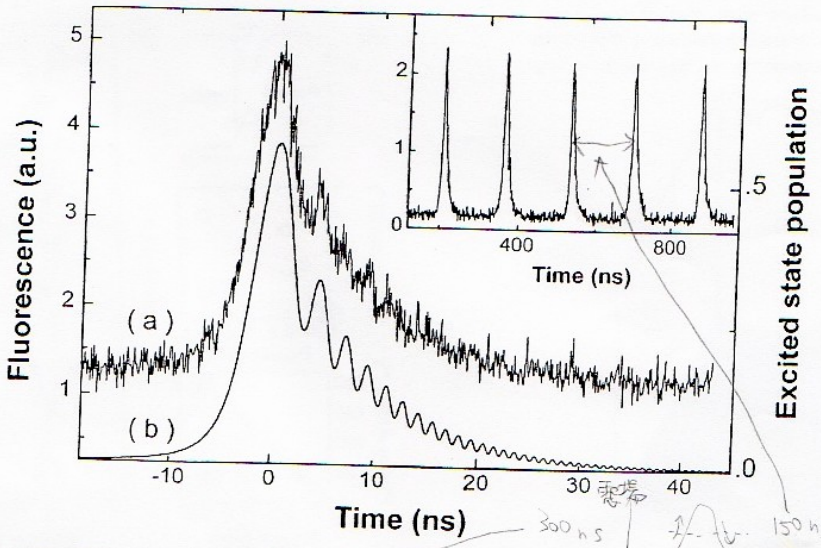

FIG. 2. Inset: fluorescence bursts of a single molecule under periodic linear Stark shifting by a sinusoidal rf wave, with cw laser excitation at a fixed frequency in the middle of the swept interval. Photon bursts are obtained whenever the molecular line crosses resonance with the laser. The rf frequency is 3 MHz and the Rabi frequency is $\Omega = 2.6\Gamma$. The molecular frequency sweeps $\Delta_0 = 90\Gamma$ ($\Gamma = 20$ MHz). The data were accumulated over 480 s. Curve (*a*) the figure shows the detailed shape of a fluorescence burst for a different set of parameters ($\nu_{rf} = 4$ MHz, $\Omega = 3\Gamma$, and $\Delta_0 = 160\Gamma$). Curve (*b*) is the burst shape from a quantum Monte Carlo simulation with the same parameters.

Triggered Source of Single Photons based on Controlled Single Molecule Fluorescence

Christian Brunel, Brahim Lounis, Philippe Tamarat, and Michel Orrit
Centre de Physique Moléculaire Optique et Hertzienne, CNRS et Université Bordeaux I, 351 Cours de la Libération, 33405 Talence, France
(Received 11 February 1999)

We use the method of adiabatic following to prepare a single molecule in its fluorescing excited state. Spontaneous emission from this state gives rise to a single photon. With our current experimental conditions, up to 74% of the sweeps lead to the emission of a single photon. Since the adiabatic passage is done on command, the molecule performs as a high rate source of triggered photons. The experimental results are in quantitative agreement with quantum Monte Carlo simulations.

Observation of Autler-Townes Splitting of Biexcitons in CuCl

Ryo Shimano and Makoto Kuwata-Gonokami*
Department of Applied Physics, Faculty of Engineering, The University of Tokyo, 7-3-1 Hongo, Bunkyo-ku, Tokyo 113, Japan
(Received 18 October 1993)

Wave-vector–selective ac Stark effect of the Γ_1-biexciton state is clearly observed in the steady

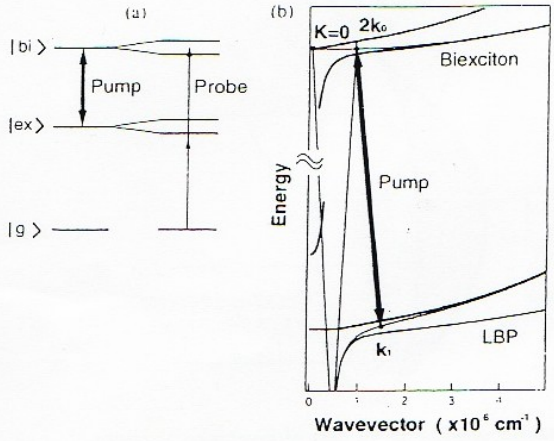

FIG. 1. (a) Schematic level diagram of the exciton and biexciton system. The exciton and biexciton states are coherently mixed by the resonant pump field. The resulting dressed states are probed by two-photon polarization (TPP) spectroscopy. (b) Calculated Autler-Townes splitting taking into account the exciton-polariton effect with spatial dispersion. The pump field mixes the lower branch polariton (LBP) with the biexciton branch. TPP spectroscopy probes the $\mathbf{K} = 2\mathbf{k}_0$

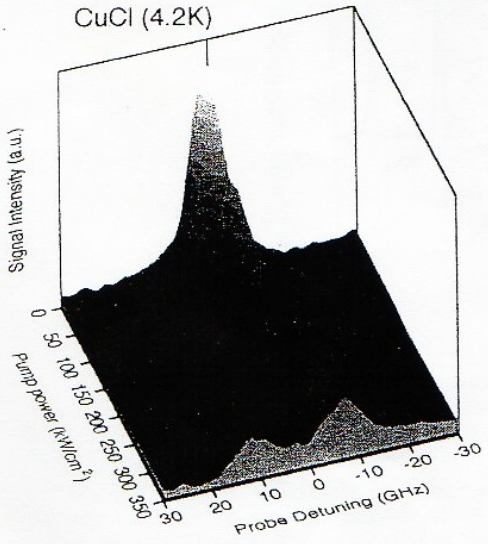

FIG. 2. TPP spectra around the biexciton line, 3.186 eV, for various pump powers. The pump detuning is almost zero.

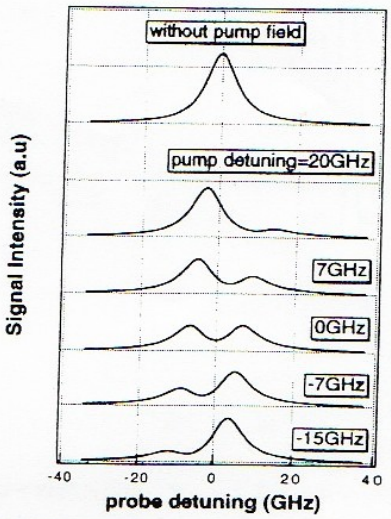

FIG. 3. Calculated TPP spectra around the biexciton line for various pump laser detunings. The biexciton dephasing

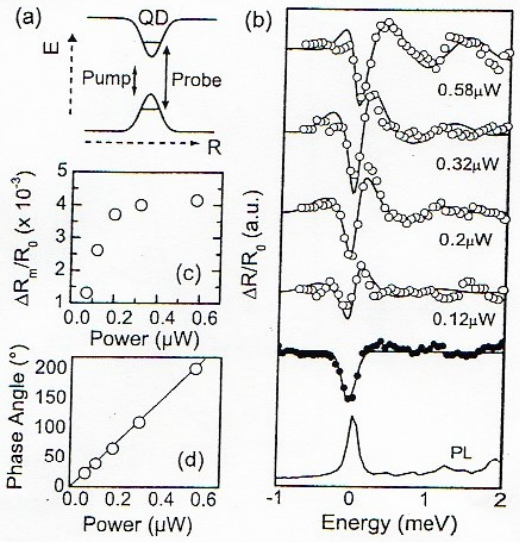

FIG. 1. (a) Schematic energy diagram. (b) PL spectrum of a single QD resonance $\omega_{QD} = 1.6503$ eV and differential reflectivity $\Delta R(\omega)/R_0$ for above band gap excitation at $\Delta t = 50$ ps (solid circles). Open circles: $\Delta R(\omega)/R_0$ for below band gap excitation at $\Delta t = -4$ ps with 2 ps pulses at 1.647 eV ($\sigma =$

Optical Stark Effect in a Quantum Dot: Ultrafast Control of Single Exciton Polarizations

Thomas Unold,[1] Kerstin Mueller,[1] Christoph Lienau,[1,*] Thomas Elsaesser,[1] and Andreas D. Wieck[2]
[1]*Max-Born-Institut für Nichtlineare Optik und Kurzzeitspektroskopie, D-12489 Berlin, Germany*
[2]*Lehrstuhl für Angewandte Festkörperphysik, Ruhr-Universität Bochum, D-44870 Bochum, Germany*
(Received 30 October 2003; published 16 April 2004)

We report the first experimental study of the optical Stark effect in single semiconductor quantum dots (QD). For below band gap excitation, two-color pump-probe spectra show dispersive line shapes caused by a light-induced blueshift of the excitonic resonance. The line shape depends strongly on the excitation field strength and is determined by the pump-induced phase shift of the coherent QD polarization. Transient spectral oscillations can be understood as rotations of the QD polarization phase with negligible population change. Ultrafast control of the QD polarization is demonstrated

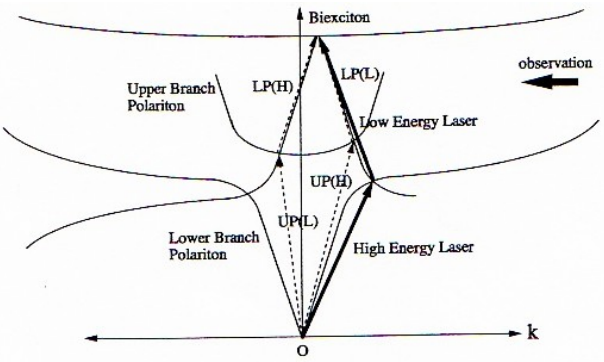

FIG. 1. The schematic of the excitation (thick solid arrow) of biexcitons near $K_m=0$ and the emissions (dashed arrow) shown with respect to the biexciton and polariton-dispersion curves. To show correctly the directions of the polariton wave vectors under the momentum conservation, the upward arrows are used for both excitation and emission processes. The LP(H) and UP(H) emissions are emitted in the observation direction while the LP(L) and UP(L) emissions are observed by internal reflection on the back surface.

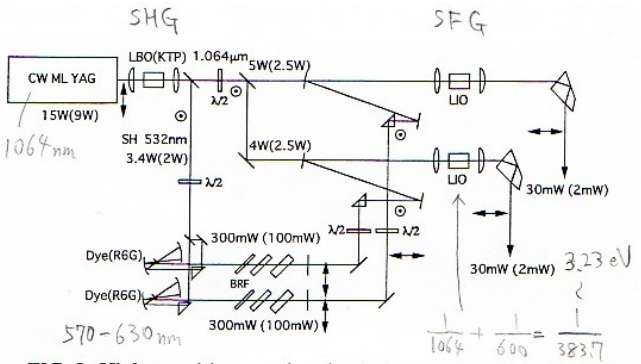

FIG. 3. High-repetition synchronized two-color tunable picosecond uv laser. The powers are improved from those in the previous paper (Ref. 33) shown in the parentheses. BRF, birefringent filter; λ/2, half-wave plate; ↔, horizontal polarization; ⊙, vertical polarization.

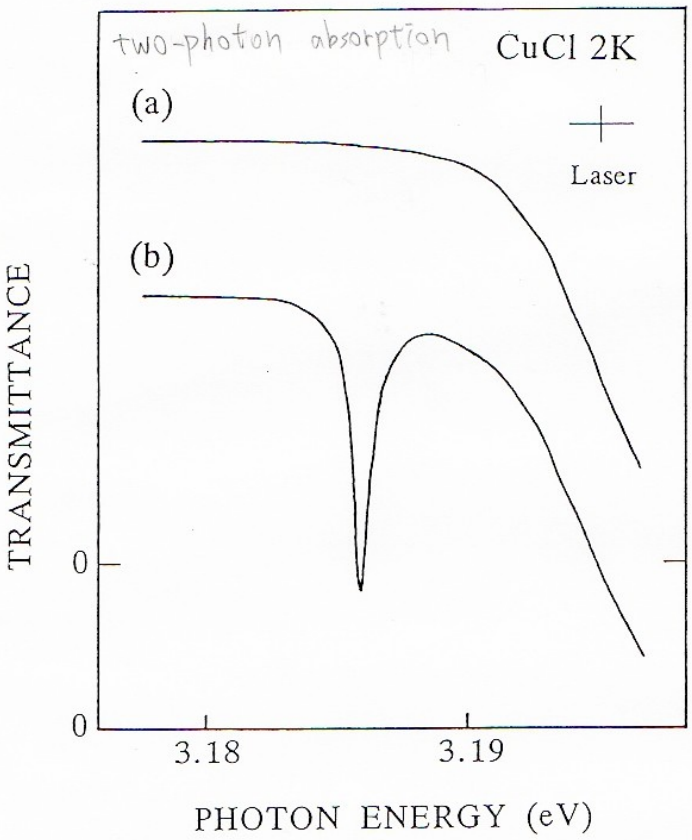

Fig.1-9 Transmission spectra around the GTA band of CuCl obtained with a circular polarized single laser beam (a) and a linear polarized single laser beam (b) at 2K
The intensity of the excitation light was 4MW/cm^2.

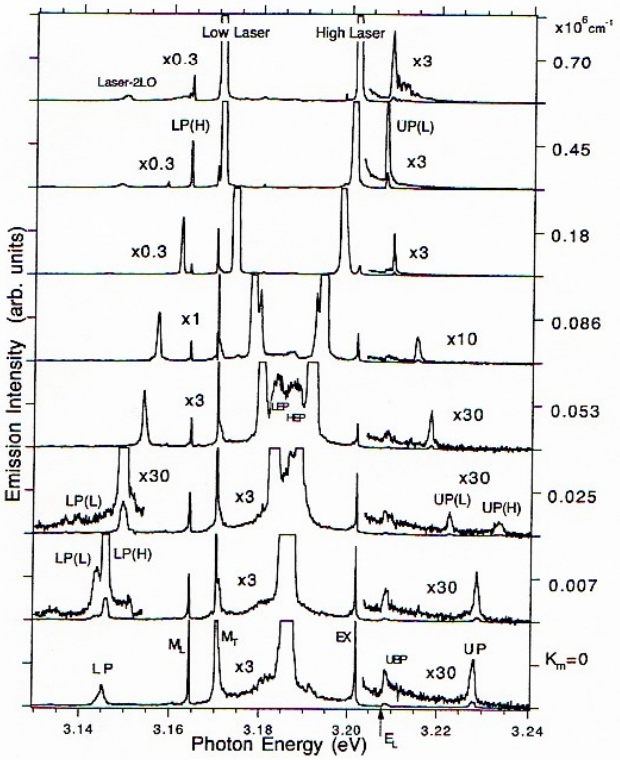

FIG. 5. Biexciton emission spectra for the wave numbers from $K_m=0$ to 0.70 ($\times 10^6$ cm^{-1}). The LP(L,H), UP(L,H) emissions are from $k_1^{(0)}-k_2^{(0)}$ biexcitons and the M_T, M_L, EX, LEP, and HEP emissions are from $\simeq k_1^{(0)}+k_2^{(0)}$ biexcitons. The longitudinal exciton energy is denoted by E_L. The emissions labeled by UBP are attributed to polaritons distributed in the upper-polariton branch as a result of the intraband relaxation of the UP polaritons.

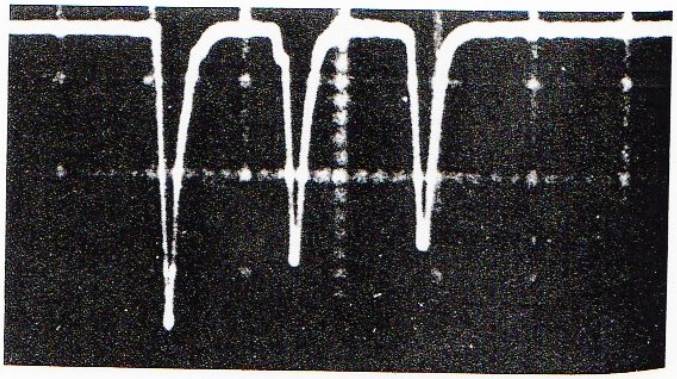

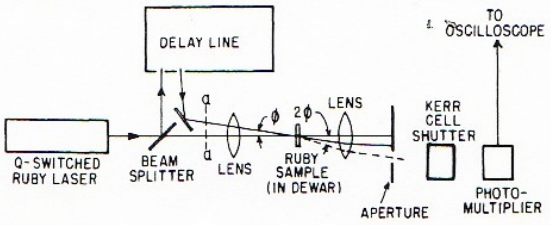

FIG. 2. Schematic experimental arrangement.

photon echo

Fig. 21.8 Oscilloscope trace (100 nsec/division) showing the photon echo from a ruby sample at 4.2 K. The echo appears as the third pulse following the two exciting pulses from a ruby laser. (After Ref. 12.)

stimulated photon echo

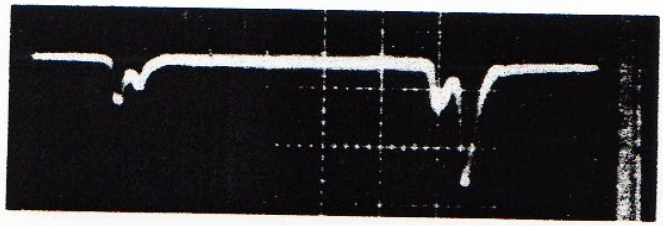

FIG. 1. Oscilloscope trace showing scattered light from three excitation pulses (third row of the table in Fig. 3 with $\vec{K}' \cdot \vec{z}/|\vec{K}'| = -1$) and the subsequent SP echo (fourth pulse) pronounced on the $3S$-$3P_{1/2}$ transition of Na when the second-to-third pulse separation is $\cong 17$ times the 16-nsec lifetime of the $3P_{1/2}$ state. At the time of the third pulse a negligible $\cong 10^{-8}$ of the intially excited population remains in the $3P_{1/2}$ state. The echo persists because of the information stored in the ground state alone. (Horizontal: 50 nsec/div.)

248-Bit optical data storage in Eu^{3+}:$YAlO_3$ by accumulated photon echoes

M. Mitsunaga and N. Uesugi

NTT Basic Research Laboratories, Musashino-shi, Tokyo 180, Japan

Received August 18, 1989; accepted October 26, 1989

The successful storage and retrieval of 248-bit temporal optical data in Eu^{3+}:$YAlO_3$ by accumulated photon echoes is reported. Owing to the long storage time of this crystal, the input data can be written bit by bit by quickly varying the separation of two laser pulses, while the stored data are recalled simultaneously after some storage period, which extends up to a few hours. The maximum data length, previously thought to be limited by the optical dephasing time T_2, has been found to be four times shorter than T_2 and attributable to spectral diffusion.

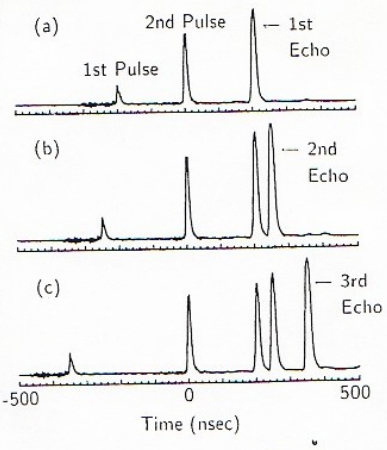

Fig. 1. Bit-by-bit writing of the optical data using accumulated photon echoes. (a) The first pulse and the second pulse are located at $t_1 = -200$ nsec and $t_2 = 0$, respectively, and a first echo is observed at $t_e = 200$ nsec. (b) The first pulse is suddenly shifted to $t_1 = -250$ nsec, and an additional echo appears. (c) The first pulse is further shifted to $t_1 = -350$ nsec, creating a third echo.

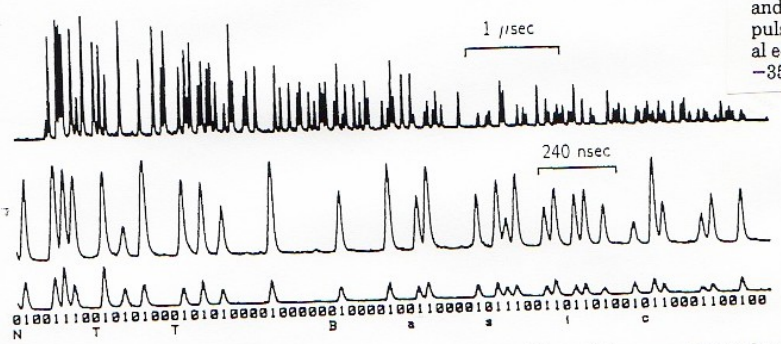

photon echo の応用

Fig. 2. Photon-echo signal for Eu^{3+}:$YAlO_3$ corresponding to the 248-bit optical input data representing the term "NTT Basic Research Laboratories." Top trace: the complete data; the storage time is 10 sec. Middle trace: the leading portion of the above signal. Bottom trace: the echo signal for the same input data as the middle trace but recalled after 2 h of storage time. The binary values and decoded characters are shown at the bottom. The vertical scales are the same for the two lower traces.

Holographic motion picture by $Eu^{3+}:Y_2SiO_5$

M. Mitsunaga and N. Uesugi

NTT Basic Research Laboratories, Atsugi-shi, Kanagawa 243-01, Japan

H. Sasaki and K. Karaki

Olympus Optical Company Ltd., Hachioji-shi, Tokyo 192, Japan

Received November 15, 1993

Real-time recording of a moving object was made with persistent spectral hole burning of a cryogenic $Eu^{3+}:Y_2SiO_5$ crystal. In a basic holographic configuration the ultrastable laser frequency was continuously scanned within the $^7F_0-^5D_0$ absorption line (typically 200 MHz in 20 s) while the object was in motion, thus permitting the storage and reconstruction of the moving image. The success of this motion picture is attributable to (1) the kilohertz-wide hole width, (2) the quasi-persistent hole lifetime, and (3) the high hole-burning quantum efficiency of this material.

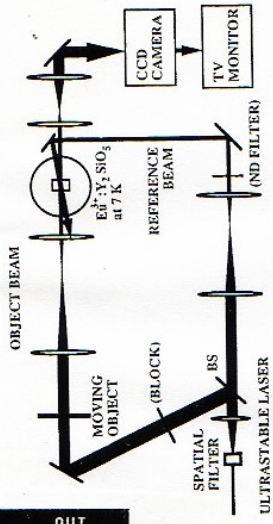

Fig. 2. Experimental setup for the holographic motion picture. BS, beam splitter; ND, neutral-density. The components in parentheses were used only for the reading stage.

hole burning の応用

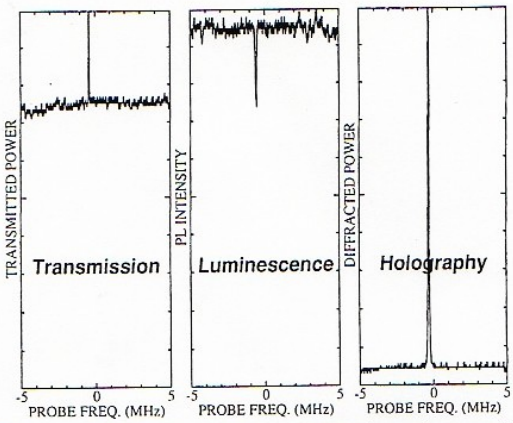

Fig. 1. Hole-burning spectra obtained by various read-out methods—transmission, luminescence, and holography—for the $^7F_0-^5D_0$ transition of $Eu^{3+}:Y_2SiO_5$ at $T = 7$ K. First, a hole was burned by application of a burn laser of a fixed frequency for 50 ms. Then the probe laser was scanned only once (no averaging) while the transmitted power, the photoluminescence (PL) intensity, and the diffracted power were detected for each measurement.

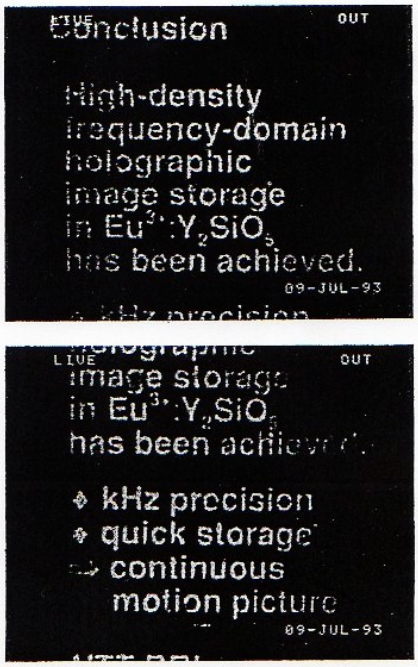

Fig. 3. Two typical stills from the reconstructed moving image.

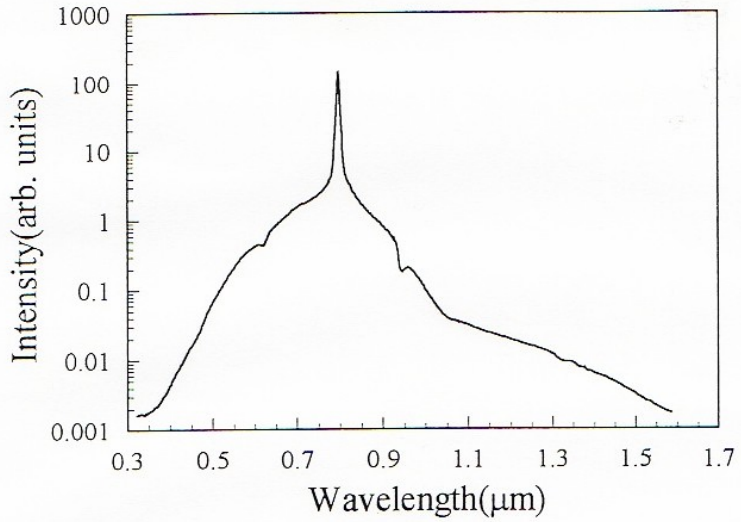

self-phase modulation

図3-1　自己位相変調により発生したフェムト秒白色光のスペクトル。中心波長0.8μm、パルス幅160fs、パルスエネルギー約0.2mJの光パルスを水または四塩化炭素中（光路長10mm）にf= 80mmのレンズで集光した。波長1.05μm以下は水を、それ以上の波長領域は四塩化炭素を用いて測定し、両者を接続して表示してある。波長0.62μmに見られる構造は、水のOH伸縮振動によるラマン散乱であり、0.94μmに見られる凹みは水自身の吸収によるものである。1.3μm以上では吸収が強いため、水は使えない。白色光のスペクトルは0.3μmの近紫外から1.6μmの近赤外域まで広がっている。

Triggered source of single photons …

DBATT　(dibenzanthanthrene) in a *n*-hexadecane matrix at 1.8K